Spectroscopy of zigzag single-walled carbon nanotubes: Comparing femtosecond transient absorption spectra with *ab initio* calculations

Ying-Zhong Ma,[1] Catalin D. Spataru,[2] Leonas Valkunas,[1,3] Steven G. Louie,[2] and Graham R. Fleming[1,*]
[1]*Department of Chemistry, University of California, Berkeley and Physical Biosciences Division, Lawrence Berkeley National Laboratory, Berkeley, California 94720-1460, USA*
[2]*Department of Physics, University of California at Berkeley, Berkeley, California 94720, USA and Materials Sciences Division, Lawrence Berkeley National Laboratory, Berkeley, California 94720, USA*
[3]*Institute of Physics, Savanoriu Ave. 231, 02300 Vilnius, Lithuania and Theoretical Physics Department, Faculty of Physics of Vilnius University, Sauletekio Ave. 9, build. 3, 10222 Vilnius, Lithuania*
(Received 10 April 2006; revised manuscript received 23 June 2006; published 8 August 2006)

Femtosecond transient absorption spectroscopy was applied to map out the electronic transition energies of a selected semiconducting zigzag carbon nanotube, the (11,0) tube. The experiment was performed by resonant excitation of the lowest electronic transition with spectrally narrow pump pulses, ensuring predominant selection of the desired tube type from a mixture of various species. We found that the lowest and the second electronic transitions are characterized by induced transmission bands peaking at 1042 and 741 nm, respectively. The association of the resolved spectral bands to the two lowest electronic transitions of the (11,0) tube was further verified by examining the corresponding kinetic profiles. Results of *ab initio* calculations are also presented for comparing the transition energies and for explaining the transient absorption kinetics detected at different wavelengths.

DOI: 10.1103/PhysRevB.74.085402 PACS number(s): 78.47.+p, 71.35.−y

I. INTRODUCTION

Zigzag nanotubes are a group of single-walled carbon nanotubes (SWNTs) with the chiral angle (θ) equal to zero.[1,2] These nanotubes are commonly selected as prototypes for elucidating theoretically the electronic structures of SWNTs because their unit cells are substantially smaller than those of chiral SWNTs ($0° < \theta < 30°$) with similar diameters, thus greatly reducing the computational effort.[3–5] A wealth of results obtained with various theoretical approaches has been reported.[3–10] In contrast, experimental assessment of the electronic structures of semiconducting zigzag nanotubes using optical spectroscopy has been hampered due to the difficulty of detecting their fluorescence emission,[11,12] and as a consequence our knowledge of their electronic transition energies comes largely from an empirical formula based on experimental data for chiral nanotubes.[13] The difficulty in observing fluorescence has been considered as an indication of preferential formation of chiral nanotubes. Alternative explanations for this phenomenon were made recently, suggesting either an exciton resonance effect,[14] or possible involvement of a dark excitonic state below the first optically allowed exciton state (E_1).[5,15]

The presence of zigzag nanotubes in the SWNT material synthesized by high-pressure catalytic decomposition carbon monoxide (HiPco) was observed by resonant Raman spectroscopy.[16,17] Owing to a significantly enhanced electron-phonon coupling in zigzag tubes, their characteristic radial breathing modes can be readily distinguished from those species with larger chiral angles. By measuring the integrated Raman intensity as a function of excitation energy, Telg *et al.* obtained the energy of the second excitonic state (E_2) of a peculiar zigzag nanotubes, (11,0) tube.[16] Experimental evidence for the presence of the (11,0) tube was also found by Jones and coworkers using steady-state fluorescence spectroscopy.[18] As its emission is weak in comparison to those chiral tubes emitting at the same spectral region, a delicate decomposition had to be performed in order to identify the spectral features associated with this peculiar tube type and to extract the E_1 and E_2 energies.[18]

A subset of semiconducting zigzag tubes including the (11,0) are characterized by $E_2/E_1 < 2$,[13] which excludes the proposed exciton resonance effect[14] as a physical mechanism for the weak or negligible emission phenomenon. Other possible causes for the weak emission are low content in the preparations or some intrinsic relaxation mechanisms or both. To explore this further, an alternative spectroscopic technique to fluorescence spectroscopy is highly desirable. In this paper, we report the results obtained for the (11,0) zigzag tube, using femtosecond transient absorption (TA) spectroscopy, which is capable of detecting both emissive and dark states. The experiment was performed using an individual nanotube-enriched HiPco-SWNT preparation suspended in aqueous solution of sodium dodecyl sulfate (SDS) micelles, permitting to access spectrally distinct tube types.[11,13,19] By purposely narrowing the bandwidth of pump pulse resonant with the E_1 state, we successfully realized *predominant* excitation of the (11,0) tube from a mixture of various tube species. In addition to the determination of the respective E_1 and E_2 energies, combination of *ab initio* calculations of the electronic structure and the experimental results enabled us to gain new insights into this unresolved issue. The dynamic behavior of this zigzag tube will be further discussed against chiral species.

II. THEORETICAL AND EXPERIMENTAL APPROACHES

The electronic structure and optical response of the (11,0) tube was calculated using an *ab initio* approach which in-

clude quasiparticle self-energy[20] and electron-hole interaction[21] effects. We refer to the previous work by Louie and coworkers for the description of the method and related technical details as applied to the carbon nanotubes.[3,4,15,22]

The SWNT material was produced by a HiPco-type generator, and the same procedure as described previously was used to prepare a sample rich in individual nanotubes in a surfactant-water system (SDS in H_2O).[23] Typical sample optical densities at the relevant spectral region were about 0.15 per mm. During data acquisition, the 1 mm path length sample cell was periodically translated within the focal plane. Stability of the sample was checked by recording the linear absorption spectra before and after the time-resolved measurements, which showed no observable change.

Femtosecond frequency-resolved TA measurements were performed using a commercial regenerative Ti:sapphire amplifier with a repetition rate of 250 kHz, generating ~50 fs (full width at half maximum, FWHM) pulses centered at ~800 nm.[24,25] An optical parametric amplifier was used to generate pump pulse resonant with the E_1 state of the (11,0) nanotube. In order to minimize direct excitation of other tube species aside from the (11,0), a 10 nm (FWHM) bandpass filter with a central wavelength of 1040 nm was introduced into the pump beam for most of the measurements. A white-light continuum served as a broadband probe, which was detected using a Peltier cooled CCD camera. A more detailed description of the experimental method can be found in Ref. 19.

To measure weak TA signals with an enhanced signal-to-noise ratio, we applied an alternative approach to probe the change of absorbance at selected wavelengths as a function of the time delay between pump and probe pulses. The detection scheme in this case consists of a monochromator, a pair of silicon photodiodes and lock-in amplifiers. A set of data collected at different wavelength under identical experimental conditions was further used to reconstruct a TA spectrum. In both the broadband and the single-wavelength probing experiments, the polarization of the pump beam was set to the magic angle (54.7°) with respect to the probe beam.

III. RESULTS

A. Theoretical

As reported previously for the (8,0) nanotube,[3,4] the *ab initio* calculations of the (11,0) tube with inclusion of the electron-hole interactions give rise to a series of exciton transitions. The energies of the E_1 and E_2 excitons are at 1.21 and 1.74 eV, and the corresponding exciton binding energies are 0.76 and 0.73 eV.[15,22] In addition to these optically allowed exciton bands, an even larger number of optically dark states is found. Figure 1 shows the series of excitonic states associated with the lowest intersubband transitions. In analogy to the energy levels in a one-dimensional (1D) hydrogen atom,[26] these states form subgroups corresponding to a different principal quantum number ($n=0,1,2,\ldots$) and symmetry (the exciton envelope function is either even or odd with respect to $z\rightarrow -z$ where the z direction is along the tube axis[27,28]). Each subgroup is comprised of four excitonic states, arising from the double degeneracy of the valence and conduction band in the zigzag nanotubes.[1] The electron-hole interactions further lead to not only removal of the degeneracy but also redistribution of oscillator strengths between the resulting excitonic states. While all states in the subgroups with odd symmetry are optically dark, some of the states with even symmetry are optically allowed. For instance, the second state in the 1*g* subgroup (see Fig. 1), which is located at 1.71 eV, also carries substantial oscillator strength.[22]

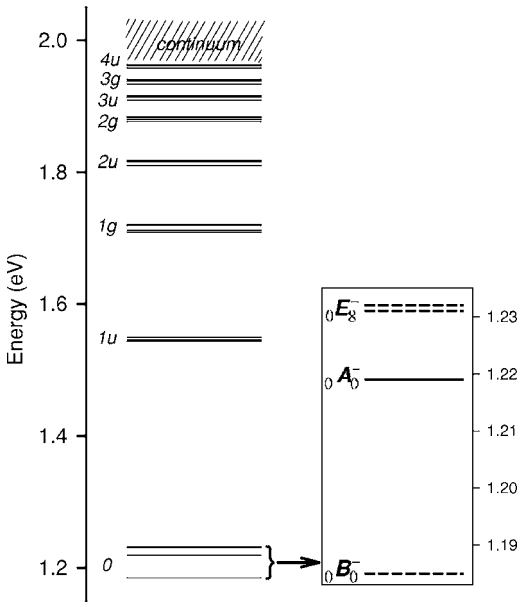

FIG. 1. Energy diagrams of the excitonic states of the (11,0) tube obtained by *ab initio* calculations. The numbers denote the principal numbers, *u* and *g* represent odd and even symmetry, respectively. The right-handed panel shows an expanded view of the subgroup corresponding to the $n=0$ level; the optically allowed and dark states are depicted by solid and dashed lines, respectively. The $_0A_0^-$ state is referred to as the E_1 state in the experimental portion of this paper.

The lowest energy subgroup in Fig. 1 (see inset) is most relevant for the present discussion due to the presence of the state with majority of the oscillator strength, i.e., the E_1 state. In addition to this E_1 state, now labeled as $_0A_0^-$ according to the notation of Damnjanovic and coworkers,[27,29] theory predicts that there are three optically dark states in this complex:[15] the $_0B_0^-$ exciton which is the lowest spin-singlet exciton in the electronic spectrum of the (11,0) tube, and the doubly degenerate higher-lying excitons $_0E_8^-$. The calculated energy difference between the $_0A_0^-$ and $_0B_0^-$ states is 29 meV.

B. Experimental

1. Spectroscopic identification of the (11,0) nanotube

The micelle-dispersed sample used in this work contains over 50 types of metallic and semiconducting nanotubes with severely overlapping absorption bands. As a result, the broad pulse spectrum of a sub-100 fs pump pulse will unavoidably excite multiple tube species, resulting from resonance with either the excitonic states of relevant tubes or their phonon

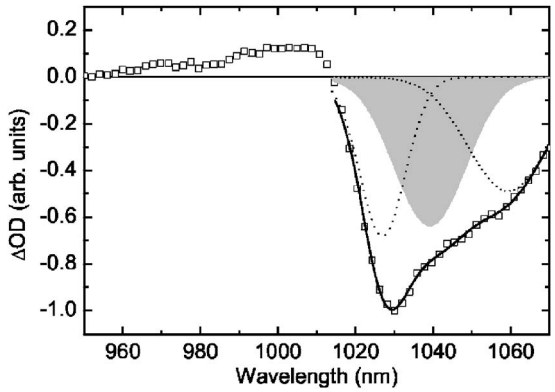

FIG. 2. The TA spectrum recorded with spectrally wide pulses centered at 1037 nm at a delay time of 70 fs. The three Gaussian components resulting from spectral deconvolution are shown in dashed lines and the fit is given by the solid line. The shaded area shows the Gaussian band associated with the (11,0) and/or (8,1) tubes.

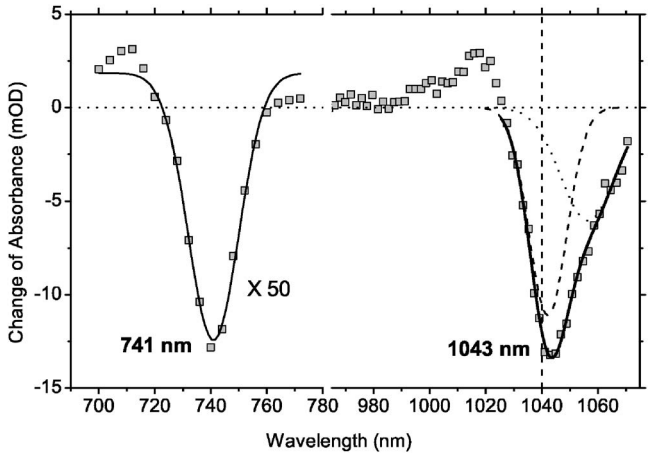

FIG. 3. The TA spectra measured in the spectral region corresponding to the E_1 and E_2 transitions of the (11,0) tube upon excitation at 1040 nm with spectrally narrow pump pulses. The spectral was recorded at a delay time of 190 fs with a pump fluence of 4.73×10^{13} photons/pulse cm^2. The solid line drawn over the experimental data collected at shorter wavelength represents a Gaussian fit. Deconvolution of the spectrum obtained at longer wavelength results in two Gaussian components (dashed and dotted lines), and the solid line is the fit of the spectrum. The vertical dashed line indicates the center frequency of the pump pulses and the horizontal dotted line is the baseline of the spectra (ΔOD=0).

subbands.[30,31] As demonstrated previously,[19,25] spectrally selective detection of a desired nanotube type is attainable in femtosecond TA experiments, provided that the E_1 energy of the tube is sufficiently distinct. However, when the excited nanotube species are associated with strongly overlapped absorption bands, spectral selection becomes difficult, and careful discrimination is needed in order to identify unambiguously a desired tube type.

Figure 2 shows the TA spectrum measured using pump pulses centered at 1037 nm, the empirically predicted wavelength for the E_1 transition of the (11,0) tube,[13] at a delay time of 70 fs. The wide spectrum associated with the $\sim$100 fs pump pulse (>20 nm, FWHM) results in a broad, asymmetry induced transmission (IT) band at wavelength longer than 1015 nm and a weak induced absorption (IA) feature at shorter wavelength. The presence of several tube species in this spectral region[13] means that the observed broad IT band contains strong contributions from multiple, structurally distinct nanotubes. According to Weisman *et al.*,[13] the contributing species may include (7,5), (8,1), (11,0), and (10,2) nanotubes, with their corresponding E_1 transitions located at 1024, 1041, 1037, and 1053 nm, respectively. Approximate assessment of the contributing species is made by spectral decomposition of this IT band, assuming a Gaussian line shape for each tube type. This decomposition results in three Gaussian bands peaked at 1027, 1039, and 1059 nm with corresponding width (FWHM) of 14, 22, and 24 nm, respectively. While this decomposition appears arbitrary, we found that the resulting peak positions do coincide reasonably well with the E_1 transition energies of the (7,5), (11,0), and/or (8,1),[32] and (10,2) tubes. In addition, the widths of the 1039 and 1059 nm bands match fairly well with the typical bandwidth of steady-state fluorescence emission spectra of semiconducting nanotubes.[23] The Gaussian band at 1027 nm appears exceptional because of its noticeably narrower bandwidth, arising most probably from a superposition with a positive-signed IA signal at wavelengths <1015 nm. Nevertheless, the generally good match between the results of our spectral decomposition and the previous steady-state fluorescence data validates this simple approach of spectral analysis for identifying nanotubes with highly overlapped absorption bands. It is pertinent to mention here that the same approach was applied by Jones and coworkers to analyze the nanotube species that contribute to the steady-state fluorescence emission spectra in this region, although a Voigt function was used instead for the line shape.[18]

While it is possible to identify the (11,0) tube from the spectral decomposition of the TA spectrum shown in Fig. 2, the severely overlapping bands of different tube species prevent further confirmation of this tube type, and spectroscopic assessment of its dynamics and electronic structure. A simple solution to this problem is to narrow the width of the pump pulse spectrum, and this is achieved by introducing a spectrally narrow bandpass filter, with a central wavelength of 1040 nm and a FWHM of 10 nm, into the pump beam. All the data presented in the reminder of this paper were obtained with this spectrally narrow pump pulse. Figure 3 shows the TA spectrum recorded at a delay time of 200 fs. This spectrum peaks at 1043 nm and has a significantly narrower bandwidth than the one shown in Fig. 2, indicating excitation of a smaller number of tube species (see Fig. 1). Assessment of the contributing tubes is again obtained by spectral decomposition, resulting in two Gaussian bands with peak positions at 1042 and 1057 nm and widths of 16 and 23 nm, respectively. These two Gaussian bands can be readily attributed to (11,0) and/or (8,1),[32] and (10,2) tubes, respectively.[13] By comparing the results of our spectral decomposition shown in Figs. 2 and 3 it is clear that use of the spectrally narrower pump pulses eliminates direct excitation of the (7,5) tube, and allows preferential excitation of the (11,0) and/or (8,1) tubes. This preferential selection is evi-

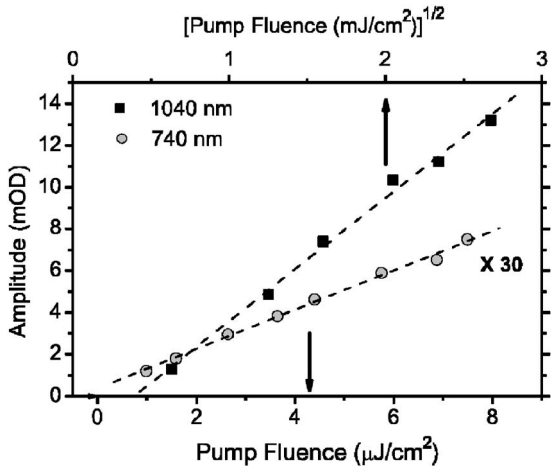

FIG. 4. The change of the maximum amplitude of the transient absorption kinetics at 740 nm (circles) and 1040 nm (squares) with the intensity of pump pulses at 1040 nm, plotted as a function of the intensity (circles vs bottom axis) or its square root (squares, top axis). The dashed lines represent the linear fits of the data.

dent from the remarkably larger amplitude of the 1042 nm Gaussian band than that of the 1057 nm (see Fig. 3).

The next step of our spectroscopic identification is to distinguish, between the (11,0) and (8,1) tubes. Although these two nanotubes have similar E_1 transition energies, their E_2 energies are very different, located at 745 and 471 nm, respectively, according to calculations using an empirical formula.[13] If the (11,0) tube is indeed excited by the 1040 nm pump pulses, an unique spectroscopic response at the corresponding E_2 transition is expected. As we have demonstrated recently,[25] optical excitation of the E_1 transition of a given semiconducting nanotube with moderate or high intensity femtosecond pulses will induce a nonlinear exciton-exciton annihilation process as the result of simultaneous generation of multiple excitons in a single tube. Kinetics caused by this relaxation process has also been observed by other groups using either femtosecond pump-probe[33] or time-resolved fluorescence techniques.[34] This nonlinear annihilation involves rapid relaxation of one exciton by releasing its energy to the second exciton, and consequently promoting the latter to an higher energy excited-state. The subsequent relaxation can result in population of the corresponding E_2 state, and thus produce a unique spectroscopic response in that spectral region. A spectroscopic response at the E_2 state may also originate from its intrinsic correlation with the E_1 state, because they have the same ground state whose photobleaching is observable at both E_1 and E_2 wavelengths. Figure 3 shows the TA spectrum obtained at a delay time of 200 fs in the region of 700–772 nm, which was reconstructed from the kinetic data collected at 19 different probing wavelengths. This spectrum is dominated by an IT band, peaked at 741 nm with a width (FWHM) of 22 nm. To test that this spectroscopic response may be indeed related to the annihilation of the (11,0) E_1 excitons, we further examined the pump intensity dependence of the maximal amplitude of the kinetics probed at 740 and 1040 nm and the results are shown in Fig. 4. In consistence with our previous analysis,[25] the corresponding amplitudes scale linearly with the pump intensity and its square root, respectively. This intensity dependence is expected as long as the relaxation from the higher-lying excited state (populated via the annihilation of the E_1 excitons) to the E_2 state, and from the E_2 to the E_1 state occurs in a timescale shorter than the duration of laser pulses.[25] Support for the occurrence of exciton-exciton annihilation is obtained by estimating the number of excitons created in a single tube. Based on the pump power, the spot size of the pump beam, an absorption cross section $\sigma \approx 1.2 \times 10^6$ cm^2/mole C,[35] and a tube length of $\sim$130 nm,[23] we found on average one exciton will be created under the highest pump intensity. As the actual number of excitons created in the nanotubes within the excitation volume follows a Poisson distribution, some of the tubes will have more than 1 exciton, and consequently exciton-exciton annihilation will occur in these nanotubes. The pump-intensity-dependent decays of the kinetics at 1040 nm, described below, further confirm the occurrence of annihilation.

According to the results of spectral decomposition shown in Fig. 3, the spectrally narrow pump pulse centered at 1040 nm excites not only the (11,0) and/or (8,1) tubes but also the (10,2) tube. Unlike the (8,1) tube, the (10,2) tube has an E_2 energy similar to that of (11,0).[11,13] It is therefore possible that the spectral response observed at 741 nm may also be contributed by the (10,2) tube. However, based on the amplitudes of the two Gaussian bands shown in Fig. 3, and an assumption of equal absorption cross sections for the two species,[36] we estimate, on average, the number of excitons created in the (10,2) tube will be 10 times less than in the (11,0) tube. Accordingly, we expect very little, if any, exciton annihilation in the (10,2) tube, leading to negligible population in its E_2 state. We therefore attribute the IT band at 741 nm obtained by using the pump pulses at 1040 nm exclusively to the (11,0) tube.

As the predicted E_1 energy of the (8,1) tube (1.191 eV) is very close to the corresponding energy of the (11,0) tube, its possible contribution to the 1042 nm bleaching band (Fig. 2) needs to be examined. In a previous steady-state fluorescence experiment, Jones *et al.* observed emission from the (11,0) tube but not from the (8,1) tube,[18] suggesting that the latter has much lower emission intensity and/or content in the sample. Comparison of the kinetics measured at 740 and 1040 nm allows us to elucidate the contribution from the (8,1) tube more precisely. When the pump intensity is low enough so that the population created in the E_2 state is negligible, the kinetics detected at both the E_1 and E_2 wavelengths will be governed by the ground state recovery. As a result, we should observe the same decay behavior at both wavelengths, because they share a common ground state. The same decay behavior can be expected even if the population in the E_2 state is not negligible, provided that the population of the E_2 state decays too rapidly to be detected. This is possible because the $E_2 \rightarrow E_1$ relaxation (estimated to be 40–60 fs[19,37]) may be significantly faster than our time resolution, because of the necessary use of spectrally narrow pump pulses in this study.[38] Before comparing the kinetics detected at the E_1 and E_2 transitions, we first separately examine the pump intensity dependence of these kinetics. Figure 5(a) shows the kinetics recorded at 1040 nm at different intensities, which are scaled to an equal amplitude at a delay

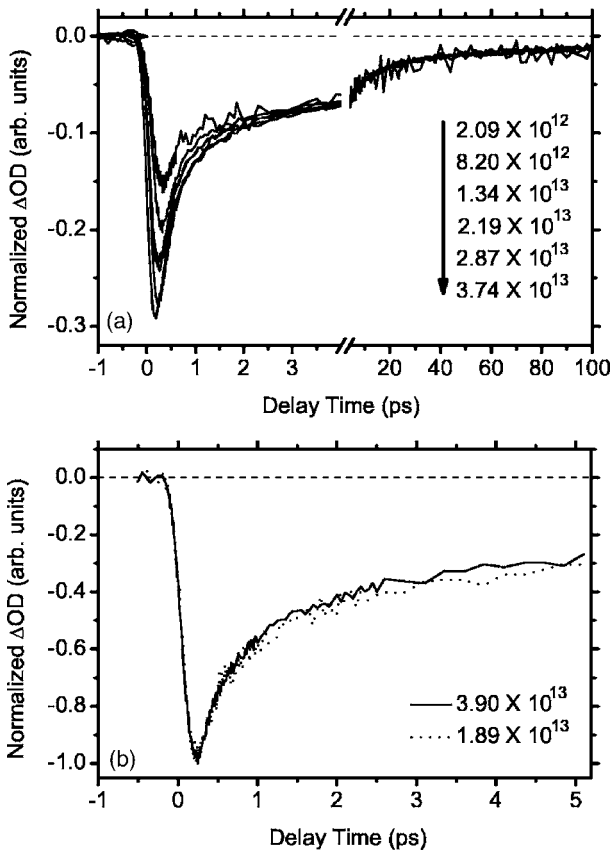

FIG. 5. (a) The TA kinetics probed at 1040 nm at different pump pulse intensities (in photons/pulse cm^2) at 1040 nm. The kinetics are scaled to an equal amplitude at 3 ps. (b) The TA kinetics probed at 740 nm at two different intensities of 1040 nm pump pulse. The kinetics are normalized at the signal maxima.

time of 3 ps. As evident from Fig. 5(a), all kinetics exhibit identical decay behavior at delay times longer than 3 ps, whereas at shorter times they are clearly dependent on the pump intensity. This dependence is manifested by the more pronounced amplitude of a fast decay component with increasing pump intensity, confirming the occurrence of exciton-exciton annihilation. In contrast, the kinetic decays at 740 nm are basically independent of the pump intensity [Fig. 5(b)]. The intensity-dependent kinetics at 1040 nm complicates somewhat the comparison of their decays with those probed at 740 nm. When the pump intensity is $>8.20\times10^{12}$ photons/pulse$\cdot cm^2$, the 1040 nm kinetics show clearly faster decay than those measured at 740 nm. However, we found the kinetics recorded at pump intensity $\leqslant 8.20\times10^{12}$ photons/pulse cm^2 exhibit an excellent match over the entire scan range of 20 ps (Fig. 6). It should be noted that, at such a pump intensity, the exciton-exciton annihilation only weakly affect the kinetics [see Fig. 5(a)]. This match means that the Gaussian band at 1042 nm (see Fig. 3) arises predominantly from the (11,0) tube, with an undetectable contribution from the (8,1) tube. This conclusion is based on a previous observation that the kinetics measured with time-resolved fluorescence and femtosecond TA spectroscopy are highly sensitive to the structure of semiconducting nanotubes,[18,24,39] and if the (8,1) tube contributes substantially, we should expect clearly different kinetics at 740 and 1040 nm.

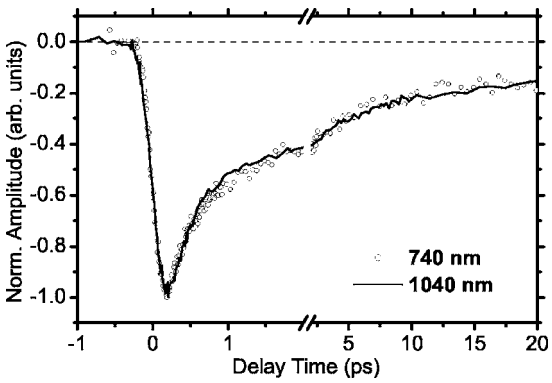

FIG. 6. Comparison of the kinetics probed at 740 (circles) and 1040 nm (solid line) upon resonant excitation with spectrally narrow pulses centered at 1040 nm. The data were collected with a pump fluence of 3.85×10^{13} and 8.20×10^{12} photons/pulse cm^2, respectively. The kinetics are normalized at the signal maxima.

2. *Characterization of the decay timescales*

We now turn to a more quantitative analysis of the kinetics that characterizes the (11,0) tube. As shown in Fig. 5(a), the exciton-exciton annihilation process ceases at delay times longer than 3 ps, analysis of the kinetics detected at 1040 nm allows determination of the lifetimes of the E_1 state of the (11,0) tube. We found that the subsequent decay follows a biexponential behavior, with lifetimes (relative amplitudes) of 8 (0.68) and 105 ps (0.32), respectively. It is pertinent to mention that the lifetime of this slower decay component matches fairly well to the result obtained by Jones *et al.* from single-photon counting measurements,[18] which was performed under a much lower excitation intensity. This similarity supports our assignment of the resolved lifetime to a characteristic time of the E_1 state.

TA kinetic profiles were also detected at 1020 nm where an IA signal dominates the TA spectrum (see Fig. 3). Similar to the data obtained at 1040 nm, these kinetics also depend on pump intensity (data not shown). Under comparable pump intensity, the kinetics recorded at 1020 and 1040 nm show an identical decay at delay times longer than 3 ps (data not shown), indicating that they likely share a common origin. At the shorter delay times, the kinetics are remarkably different: the one measured at 1020 nm shows clearly faster decay than the 1040 nm profile. To quantitatively characterize the initial rapid decay seen at 1020 nm, we preformed global lifetime analysis. In this analysis, the data collected at 1020 and 1040 nm are fitted simultaneously, where the lifetimes describing the identical decays are treated as global parameters, and the lifetime associated with the rapid decay component seen in the 1020 nm kinetics and all the amplitudes were taken as independent, free variables. In order to minimize the effect of exciton-exciton annihilation, we choose a data set measured at an intensity of $\sim 4.30\times10^{12}$ photons/pulse cm^2 for the analysis. This analysis gives a timescale of 160 fs for the rapid decay component of the 1020 nm kinetics (Fig. 7).

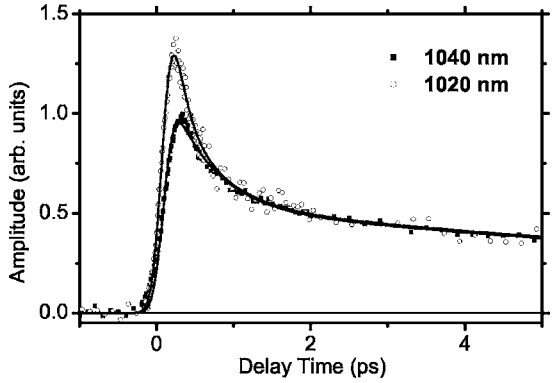

FIG. 7. Comparison of the TA kinetics at 1020 (open circles) and 1040 nm (squares) measured at a pump intensity of 4.30 $\times 10^{12}$ photons/pulse cm^2. For ease of comparison, the data collected at 1040 nm are multiplied by (−1) and are scaled to equal amplitude at 3 ps to the kinetics measured at 1020 nm. The solid lines are the results of global fitting. See text for details.

IV. DISCUSSION

A. Determination of the electronic transition energies of the (11,0) tube

We have shown in the preceding section that use of a spectrally narrow pump pulse enabled us to predominantly excite the (11,0), and two spectral bands characterizing the E_1 and E_2 states (see Fig. 3) are identified. It is now straightforward to extract the values of the corresponding transition energies from the peak positions of the corresponding IT bands shown in Fig. 3, giving $E_1=1.19$ eV and $E_2=1.67$ eV, respectively.

It is interesting to compare the E_1 and E_2 energies determined in this work with currently available values. For ease of comparison, we summarized in Table I all the available values of the E_2 and E_1 transition energies and their ratios. The energies determined here are very close to the previously empirically predicted values,[13] and the results of a very recent steady-state fluorescence experiment using a similar preparation.[18] A close similarity is also found between the E_2 energy determined in this work and the value obtained from the Raman experiment using HiPco-SWNT tubes.[16]

TABLE I. Comparison of the electronic transition energies of the (11,0) tube and their ratios determined by different methods.

	E_2 (eV)	E_1 (eV)	E_2/E_1
ab initio calculation	1.74	1.21	1.44
This work	1.67	1.19	1.41
Predicted from fluorescence[a]	1.66	1.20	1.39
Raman experiment[b]	1.66		
Fluorescence experiment[c]	1.67	1.19	1.40

[a]These values are taken from Ref. 13.
[b]This value is taken from Ref. 16.
[c]These values are taken from Ref. 18.

The transition energies obtained from the *ab initio* calculations (for an isolated tube in vacuum) are slightly higher than the experimental values by 20 and 70 meV for the E_1 and E_2 transitions, respectively. While the excitation energies from *ab initio* calculations are at the level of accuracy of ~0.1 eV, the difference between theory and experimental may also arise from dielectric screening owing to the presence of ionic SDS micelles around the tubes in the sample, resulting in a decrease of the transition energies.[40,41] It fact, it was indeed observed by Lefebvre and coworkers that the individual SWNTs suspended in air have higher E_1 and E_2 energies by, on average, 28 and 16 meV than the tubes wrapped by SDS-micelles.[42]

B. Exciton relaxation within the lowest excitonic subband

As shown in Fig. 1, *ab initio* calculations predict that the $n=0$ subgroup of excitonic states associated with the lowest intersubband transitions consists of four closely spaced levels, in which, three are optically dark. The presence of these dark states and their involvement in the exciton relaxation can affect both the TA spectra and kinetics by contributing to ground state bleaching or/and excited-state absorption. To illustrate qualitatively how this relaxation is related to our experimental observation, we consider only the ${}_0A_0^-$ and ${}_0B_0^-$ levels. Since the transition between the ground state and the ${}_0B_0^-$ state is forbidden, the ${}_0B_0^-$ state can be populated only indirectly via excitation of the ${}_0A_0^-$ state and subsequent ${}_0A_0^- \rightarrow {}_0B_0^-$ relaxation. While both the ${}_0A_0^-$ and ${}_0B_0^-$ states may give rise to IA signals, the corresponding kinetics should be very different because of the ${}_0A_0^- \rightarrow {}_0B_0^-$ relaxation, giving rise to a decay and a rise, respectively, with the same timescale characterizing the relaxation. In view of the fast decay seen at 1020 nm, we can conclude that the TA signal observed originates mainly from the ${}_0A_0^-$ state.

The overall time evolution of the exciton population will be governed by the redistribution between the ${}_0A_0^-$ and ${}_0B_0^-$ levels, and additionally by the relaxation to the ground state. At high intensity of excitation, exciton-exciton annihilation will also affect the dynamics. We neglect this nonlinear effect by focusing on the data collected at low excitation intensity (Fig. 7). The change of absorbance at a given delay time t and a probe wavelength λ is given by

$$\begin{aligned}\Delta OD(t,\lambda) &\propto (\sigma_A^{IA} - \sigma_A^{SE} - \sigma_0)n_A(t) + (\sigma_B^{IA} - \sigma_0)n_B(t) \\ &= (\sigma_A^{IA} - \sigma_A^{SE})n_A(t) + \sigma_B^{IA} n_B(t) - [n_A(t) + n_B(t)]\sigma_0, \end{aligned} \quad (1)$$

where $n_A(t)$ and $n_B(t)$ represent the exciton populations in the ${}_0A_0^-$ and ${}_0B_0^-$ levels, σ_0 is the cross section of the ground-state absorption, $\sigma_i^{SE}(\lambda)$ and $\sigma_i^{IA}(\lambda)$ are the cross sections of the stimulated emission and the IA from the ith excitonic levels, respectively, and A and B denote the ${}_0A_0^-$ and ${}_0B_0^-$ levels. From Eq. (1), it is clear that population redistribution has no effect on the bleaching of the ground state, but will influence the stimulated emission and the IA. When the probe pulse is tuned to ground state absorption band such as at 1040 nm, the kinetics may be insensitive to the population redistribution if $\sigma_A^{SE}(1040\ \text{nm})$ and $\sigma_A^{IA}(1040\ \text{nm})$ are similar.

In contrast, at 1020 nm the contributions from both the ground state bleaching and the stimulated emission from the ${}_0A_0^-$ state are small relative to the IA signal. As a result, the kinetics become more sensitive to the population redistribution, since the IA signals originating from the ${}_0A_0^-$ and ${}_0B_0^-$ levels are likely distinct spectrally. The timescale associated with the rapid decay at 1020 nm can be considered as a rough estimate for the ${}_0A_0^- \rightarrow {}_0B_0^-$ relaxation, which is 160 fs.

This rapid relaxation to the dark state will effectively decrease the fluorescence emission from the ${}_0A_0^-$ state. From the calculated energy difference between the ${}_0A_0^-$ and ${}_0B_0^-$ states it can be readily estimated that about 2/3 of the exciton population will be at the dark state, if the thermalization timescale is shorter or comparable to the ${}_0A_0^- \rightarrow {}_0B_0^-$ relaxation time and the lifetime of the ${}_0B_0^-$ state is long compared to both timescales.

C. Comparison of the kinetic behavior between the (11,0) tube and chiral species

We demonstrated previously[24] that exciton-exciton annihilation is the predominant dynamical process in selected chiral tubes and is characterized by several unique spectroscopic and dynamic signatures. (1) Electronically resonant excitation of the E_1 state of the (8,3) tube at 953 nm induces an instantaneous spectral response at 660 nm, the location of the corresponding E_2 transition. (2) The dependence of the amplitude of the transient absorption signal on the intensity of pump pulses at 953 nm differs for the kinetics probed at 660 and 953 nm. The former exhibits a linear dependence, whereas a saturating behavior is seen for the data obtained with a 953 nm probe pulse. (3) The kinetics probed at 660 and 953 nm upon resonant excitation of the E_1 transition are strongly correlated with each other. This correlation is manifested by an excellent match between the squared profile of the kinetics recorded at 953 nm and the kinetics measured at 660 nm. (4) A decay behavior independent of the pump intensity is observed for the kinetics probed at 953 nm. These observations were ascribed to the creation of a high exciton population in the chiral nanotubes, and to precise cancellation of the ground state bleaching at the E_2 transition by the induced absorption from E_1. In comparison, the kinetic decays observed for the (11,0) tube are clearly dependent on the excitation intensity [see Fig. 5(a)]. In addition, the kinetics detected at 740 nm appear identical to the data probed at 1040 nm with pump intensities $\leqslant 8.20 \times 10^{12}$ photons/pulse cm^2. We believe that the different kinetic behavior observed for the (11,0) tube results from a remarkably low population of excitons created due to the use of ~6 times lower pump power in combination with a possibly smaller absorption cross section or/and shorter length of this zigzag nanotubes. This is in line with the numerical estimate described above, showing that a majority of the excited tubes contain a single exciton even at highest excitation intensities used in the experiments.

The 1040 nm kinetics measured at high pump intensities ($>8.20 \times 10^{12}$ photons/pulse cm^2) differ from those obtained at 740 nm and is in marked contrast with the results obtained at low pump intensity. The observed difference seems to suggest that the E_1 state decays differently from the recovery of the ground state, i.e., an increase of the pump intensity is likely to predominantly affect the dynamics of the E_1 state. This could be an indication that the E_2 state is not involved in the relaxation from the highly excited states populated via exciton-exciton annihilation.[43] In this case, the annihilation taking place in the nanotube fraction that initially contains more than one exciton will affect only the 1040 nm kinetics, resulting in the intensity dependence shown in Figs. 4 and 5(a). The 740 nm kinetics, which probe the ground state recovery at the transition into the E_2 state, will not change with the excitation intensity.

As a final remark, we now briefly comment on the abundance of zigzag tubes in various HiPco SWNT materials. While the fluorescence emission from semiconducting zigzag nanotubes is generally absent, the presence of these tubes has been unambiguously identified by previous resonant Raman[16,17] and our current transient absorption measurements. This result is fully consistent with the current understanding of the fluorescence intensity being not a good measure of the tube abundance, because the intrinsic fluorescence quantum yield is strongly chirality-dependent.[36] A detailed account on the recent development in quantitative characterization of the abundance of nanotube species using either fluorescence, or resonant Raman or a combination of these two, can be found in Refs. 44–46.

V. CONCLUSION

Application of femtosecond TA spectroscopy, we have experimentally resolved the spectra and kinetics characterizing the two lowest electronic transitions of the (11,0) tube. This was achieved by resonant excitation of the E_1 transition with spectrally narrow pump pulses, which minimized excitation of other unwanted tube species. The resulting TA spectrum was analyzed by simple spectral decomposition with Gaussian functions, and a dominant component peaked at 1042 nm was assigned to the E_1 transition of the (11,0) tube. The corresponding E_2 transition is characterized by a single Gaussian profile peaked at 741 nm. To verify that these Gaussian profiles are indeed originated from the E_1 and E_2 transitions of the (11,0) tube, we further examined the TA kinetics at 1040 and 740 nm, as well as their dependence on excitation intensity. We found that the kinetics measured at 1040 nm under a low excitation intensity exhibits an identical decay behavior with the one probed at 740 nm, which is independent of the pump intensity. At such an intensity, the nonlinear exciton-exciton annihilation becomes minor, and identical kinetics result from the recovery of their common ground state. The identical kinetics thus provides strong support for our assignment of the two Gaussian bands. We further determined the energies for the corresponding transitions, giving $E_1 = 1.19$ eV and $E_2 = 1.67$ eV, respectively. These values match well with the results of *ab initio* calculations.

We further investigated the role of the lowest-lying dark state, the ${}_0B_0^-$ state, by quantitatively analyzing the kinetics obtained at 1020 and 1040 nm. This analysis enabled us to extract a timescale of 160 fs for the relaxation from the op-

tically allowed state ${}_0A_0^-$ to this dark state. This rapid relaxation will significantly diminish the fluorescence emission from the ${}_0A_0^-$ state, and thus can account for at least partially the weak or negligible emission from this subset of zigzag nanotubes.

ACKNOWLEDGMENTS

The work at Berkeley was supported by the NSF. C.D.S. and S.G.L. would like to acknowledge that their work was supported in part by the NSF under Grant No. DMR04-39768, and the U.S. DOE under Contract No. DE-AC03-76SF00098. Computational resources have been provided by NERSC and NPACI. L.V. thanks the Fulbright Foundation for financial support. We thank S. L. Dexheimer for helpful discussion, S. M. Bachilo and R. E. Smalley for providing the HiPco SWNT materials.

*To whom correspondence should be addressed. Email address: GRFleming@lbl.gov

[1] S. Saito, G. Dresselhaus, and M. S. Dresselhaus, *Physical Properties of Carbon Nanotubes* (Imperial College Press, London, 1998).
[2] T. W. Odom, J.-L. Huang, P. Kim, and C. M. Lieber, J. Phys. Chem. B **104**, 2794 (2000).
[3] C. D. Spataru, S. Ismail-Beigi, L. X. Benedict, and S. G. Louie, Phys. Rev. Lett. **92**, 077402 (2004).
[4] C. D. Spataru, S. Ismail-Beigi, L. X. Benedict, and S. G. Louie, Appl. Phys. A **78**, 1129 (2004).
[5] H. Zhao and S. Mazumdar, Phys. Rev. Lett. **93**, 157402 (2004).
[6] J. Cioslowski, N. Rao, and D. Moncrieff, J. Am. Chem. Soc. **124**, 8485 (2002).
[7] L. G. Bulusheva, A. V. Okotrub, D. A. Romanov, and D. Tomanek, J. Phys. Chem. A **102**, 975 (1998).
[8] V. Perebeinos, J. Tersoff, and P. Avouris, Phys. Rev. Lett. **92**, 257402 (2004).
[9] V. Perebeinos, J. Tersoff, and P. Avouris, Phys. Rev. Lett. **94**, 086802 (2005).
[10] E. Chang, G. Bussi, A. Ruini, and E. Molinari, Phys. Rev. Lett. **92**, 196401 (2004).
[11] S. M. Bachilo, M. S. Strano, C. Kittrell, R. H. Hauge, R. E. Smalley, and R. B. Weisman, Science **298**, 2361 (2002).
[12] S. Lebedkin, F. Hennrich, T. Skipa, and M. M. Kappes, J. Phys. Chem. B **107**, 1949 (2003).
[13] R. B. Weisman and S. M. Bachilo, Nano Lett. **3**, 1235 (2003).
[14] S. Reich, C. Thomsen, and J. Robertson, Phys. Rev. Lett. **95**, 077402 (2005).
[15] C. D. Spataru, S. Ismail-Beigi, R. B. Capaz, and S. G. Louie, Phys. Rev. Lett. **95**, 247402 (2005).
[16] H. Telg, J. Maultzsch, S. Reich, F. Hennrich, and C. Thomsen, Phys. Rev. Lett. **93**, 177401 (2004).
[17] M. Machón, S. Reich, H. Telg, J. Maultzsch, P. Ordejón, and C. Thomsen, Phys. Rev. B **71**, 035416 (2005).
[18] M. Jones, C. Engtrakul, W. K. Metzger, R. J. Ellingson, A. J. Nozik, M. J. Heben, and G. Rumbles, Phys. Rev. B **71**, 115426 (2005).
[19] Y.-Z. Ma, L. Valkunas, S. L. Dexheimer, and G. R. Fleming, Mol. Phys. **104**, 1179 (2006).
[20] M. S. Hybertsen and S. G. Louie, Phys. Rev. B **34**, 5390 (1986).
[21] M. Rohlfing and S. G. Louie, Phys. Rev. B **62**, 4927 (2000).
[22] J. B. Neaton, K. H. Khoo, C. D. Spataru, and S. G. Louie, Comput. Phys. Commun. **169**, 1 (2005).
[23] M. J. O'Connell, S. M. Bachilo, C. B. Huffman, V. C. Moore, M. S. Strano, E. H. Haroz, K. L. Rialon, P. J. Boul, W. H. Noon, C. Kittrell, J. Ma, R. H. Hauge, R. B. Weisman, and R. E. Smalley, Science **297**, 593 (2002).
[24] Y.-Z. Ma, J. Stenger, J. Zimmermann, S. M. Bachilo, R. E. Smalley, R. B. Weisman, and G. R. Fleming, J. Chem. Phys. **120**, 3368 (2004).
[25] Y.-Z. Ma, L. Valkunas, S. L. Dexheimer, S. M. Bachilo, and G. R. Fleming, Phys. Rev. Lett. **94**, 157402 (2005).
[26] R. Loudon, Am. J. Phys. **27**, 649 (1959).
[27] M. Damnjanović, I. Milošević, T. Vuković, and R. Sredanović, Phys. Rev. B **60**, 2728 (1999).
[28] J. Maultzsch, R. Pomraenke, S. Reich, E. Chang, D. Prezzi, A. Ruini, E. Molinari, M. S. Strano, C. Thomsen, and C. Lienau, Phys. Rev. B **72**, 241402(R) (2005).
[29] M. Damnjanović, T. Vuković, and I. Milošević, J. Phys. A **33**, 6561 (2000).
[30] S. G. Chou, F. P. Filho, J. Jiang, R. Saito, D. Nezich, H. B. Ribeiro, A. Jorio, M. A. Pimenta, Ge. G. Samsonidze, A. P. Santos, M. Zheng, G. B. Onoa, E. D. Semke, G. Dresselhaus, and M. S. Dresselhaus, Phys. Rev. Lett. **94**, 127402 (2005).
[31] V. Perebeinos, J. Tersoff, and P. Avouris, Phys. Rev. Lett. **94**, 027402 (2005).
[32] The E_1 transition energies of these two tubes are too close to be distinguished directly from spectral deconvolution.
[33] L. Huang and T. D. Krauss, Phys. Rev. Lett. **96**, 057407 (2006).
[34] F. Wang, G. Dukovic, E. Knoesel, L. E. Brus, and T. F. Heinz, Phys. Rev. B **70**, 241403(R) (2004).
[35] M. F. Islam, D. E. Milkie, C. L. Kane, A. G. Yodh, and J. M. Kikkawa, Phys. Rev. Lett. **93**, 037404 (2004).
[36] Y. Oyama, R. Saito, K. Sato, J. Jiang, Ge. G. Samsonidze, A. Grüneis, Y. Miyauchi, S. Maruyama, A. Jorio, G. Dresselhaus, and M. S. Dresselhaus, Carbon **44**, 873 (2006).
[37] C. Manzoni, A. Gambetta, E. Menna, M. Meneghetti, G. Lanzani, and G. Cerullo, Phys. Rev. Lett. **94**, 207401 (2005).
[38] For a transform-limited pulse, the product of its temporal duration and spectral bandwidth is constant, whose value depends on the pulse shape. This means that a pulse with narrow spectral width will be temporally long.
[39] T. Hertel, A. Hagen, V. Talalaev, K. Arnold, F. Hennrich, M. Kappes, S. Rosenthal, J. McBride, H. Ulbricht, and E. Flahaut, Nano Lett. **5**, 511 (2005).
[40] H. Ando, H. Oohashi, and H. Kanbe, J. Appl. Phys. **70**, 7024 (1991).
[41] R. B. Capaz, C. D. Spataru, S. Ismail-Beigi, and S. G. Louie, cond-mat/0606474 (unpublished).
[42] J. Lefebvre, J. M. Fraser, Y. Homma, and P. Finnie, Appl. Phys. A **78**, 1107 (2004).

[43] L. Valkunas, Y.-Z. Ma, and G. R. Fleming, Phys. Rev. B **73**, 115432 (2006).

[44] A. Jorio, A. P. Santos, H. B. Ribeiro, C. Fantini, M. Souza, J. P. M. Vieira, C. A. Furtado, J. Jiang, R. Saito, L. Balzano, D. E. Resasco, and M. A. Pimenta, Phys. Rev. B **72**, 075207 (2005).

[45] A. Jorio, C. Fantini, M. A. Pimenta, D. A. Heller, M. S. Strano, M. S. Dresselhaus, Y. Oyama, J. Jiang, and R. Saito, Appl. Phys. Lett. **88**, 023109 (2006).

[46] T. Okazaki, T. Saito, K. Matsuura, S. Ohshima, M. Yumura, Y. Oyama, R. Saito, and S. Iijima, Chem. Phys. Lett. **420**, 286 (2006).